

1 **A dual-biomarker approach for quantification of**
2 **changes in relative humidity from sedimentary lipid D/H**
3 **ratios**

4

5 Oliver Rach^{1,2}, Ansgar Kahmen³, Achim Brauer⁴, Dirk Sachse¹

6

7 ¹GFZ – German Research Centre for Geosciences, Section 5.1 Geomorphology, Organic Surface
8 Geochemistry Lab, Telegrafenberg, 14473 Potsdam (Germany)

9 ²Institute for Earth- and Environmental Science, University of Potsdam, Karl-Liebknecht-Strasse 24-
10 25, 14476 Potsdam (Germany)

11 ³Department of Environmental Sciences-Botany, University of Basel, Schönbeinstrasse 6, CH-4056
12 Basel (Switzerland)

13 ⁴GFZ – German Research Centre for Geosciences, Section 5.2 Climate Dynamics and Landscape
14 Evolution, Telegrafenberg, 14473 Potsdam (Germany)

15

16 *Correspondence to:* Oliver Rach (oliver.rach@gfz-potsdam.de)

17

18 **Abstract**

19 Past climatic change can be reconstructed from sedimentary archives by a number of proxies.
20 However, few methods exist to directly estimate hydrological changes and even fewer result in
21 quantitative data, impeding our understanding of the timing, magnitude and mechanisms of
22 hydrological changes.

23 Here we present a novel approach based on $\delta^2\text{H}$ values of sedimentary lipid biomarkers in combination
24 with plant physiological modeling, to extract quantitative information on past changes in relative
25 humidity. Our initial application to an annually laminated lacustrine sediment sequence from western
26 Europe deposited during the Younger Dryas cold period revealed relative humidity changes of up to
27 15% over sub-centennial timescales, leading to major ecosystem changes, in agreement with
28 palynological data from the region. We show that by combining organic geochemical methods and
29 mechanistic plant physiological models on well characterized lacustrine archives it is possible to
30 extract quantitative ecohydrological parameters from sedimentary lipid biomarker $\delta^2\text{H}$ data.

31

32 **1. Introduction**

33

34 Predicting future changes in the water cycle using state-of-the art climate models is still associated with
35 large uncertainties (IPCC, 2015). This is because we lack a mechanistic understanding of some of the
36 key processes that influence the water cycle, in particular at regional spatial scales. A better
37 mechanistic understanding of drivers and feedbacks within the hydrological cycle can be achieved from

38 reconstructing past hydrological changes from sedimentary archives. Stable isotope ratios of meteoric
39 water, expressed as $\delta^{18}\text{O}$ and $\delta^2\text{H}$ (δD) values are an excellent tool in this respect, because their
40 variability is associated with changes in temperature and source water (Bowen, 2008; Gat, 1996). The
41 isotope ratios of precipitation can be recorded in ice core (Alley, 2000), terrestrial and marine
42 paleoclimate archives through a variety of proxies, such as carbonates (Kanner et al., 2013; von
43 Grafenstein et al., 1999), silicates (Tyler et al., 2008) and lipid biomarkers (Sachse et al., 2012).

44 Despite their potential, the interpretation of the stable isotope ratios from inorganic and organic proxies
45 often allows only a *qualitative* assessment of past hydrological changes while *quantitative*
46 reconstructions of hydrological changes from isotope proxy data, such as precipitation amount or
47 relative humidity, have been difficult to achieve. This is problematic as quantifiable data are necessary
48 for identifying the mechanistic drivers of past hydroclimate changes as well as their continental scale
49 feedbacks and thresholds for example for vegetation changes. Moreover, quantitative data are needed
50 to test the performance of state-of-the art climate models in simulating past and future changes in the
51 hydrological cycle.

52 The interpretation of isotope proxies is typically not quantitative because multiple drivers can influence
53 meteoric $\delta^{18}\text{O}$ and $\delta^2\text{H}$ values, hampering the assignment of single quantitative relationships between a
54 hydrologic variable and $\delta^2\text{H}$ values recorded in a geological archive (Alley and Cuffey, 2001). The
55 increased understanding of the interplay between environmental and plant physiological factors
56 affecting lipid biomarker stable isotope ratios over the last decade (Feakins, 2013; Kahmen et al.,
57 2013a; Kahmen et al., 2013b; Sachse et al., 2009; Smith and Freeman, 2006) has resulted in significant
58 potential for quantitative paleohydrological approaches, exemplified by a reconstruction of seasonality
59 in precipitation and bog surface wetness in a Norwegian peatland (Nichols et al., 2009). Here we take
60 this a step further, combining lipid biomarker hydrogen isotope measurements and plant physiological
61 modeling to constrain the influence of multiple drivers on $\delta^2\text{H}$ values recorded in organic material and
62 thus allow the extraction of quantitative information about changes in relative humidity from
63 sedimentary archives.

64 Over the past decade, $\delta^2\text{H}$ values of lipid biomarkers from photosynthetic organisms have been
65 increasingly used as proxies for reconstructing past changes in the continental hydrological cycle
66 (Feakins, 2013; Rach et al., 2014; Sachse et al., 2012; Schefuss et al., 2011; Seki et al., 2011). In
67 particular *n*-alkanes are ubiquitous in marine and lacustrine sediments and can be preserved over
68 geological timescales (Peters et al., 2007). *n*-Alkanes can be traced back to aquatic or terrestrial
69 sources, where short-chain homologues ($n\text{C}_{17}$ - $n\text{C}_{21}$) are primarily synthesized by algae and aquatic
70 plants (Aichner et al., 2010; Ficken et al., 2000), mid-chain *n*-alkanes (e.g. $n\text{C}_{23}$ - $n\text{C}_{25}$) by submerged
71 aquatic macrophytes or mosses (Aichner et al., 2010; Ficken et al., 2000; Gao et al., 2011), and long-
72 chain *n*-alkanes ($>n\text{C}_{25}$) predominantly by higher terrestrial plants as a protective leaf wax layer on the
73 leaf surface (Bush and McInerney, 2013; Eglinton and Hamilton, 1967).

74 Algae and submerged aquatic plants directly use lake (or ocean) water as their hydrogen source for
75 lipid synthesis. $\delta^2\text{H}$ values from *n*-alkanes from aquatic organisms ($\delta^2\text{H}_{\text{aq}}$) are thus related to the $\delta^2\text{H}$
76 value of the water these organisms live in (Aichner et al., 2010; Sachse et al., 2004) offset by a
77 biosynthetic fractionation (ϵ_{bio}) between water and *n*-alkanes (Sachse et al., 2012) (Eq. (1)). Laboratory

78 culture studies (Zhang and Sachs, 2007) as well as field studies (Aichner et al., 2010; Sachse et al.,
79 2004) have resulted in strong linear and nearly 1:1 relationships between source water and $\delta^2\text{H}_{\text{aq}}$
80 (Sachse et al., 2012), but have shown that species specific differences in ϵ_{bio} do exist (Zhang and Sachs,
81 2007).

82

$$(1) \delta^2\text{H}_{\text{aq}} = \delta^2\text{H}_{\text{precip}} + \epsilon_{\text{bio(aq)}}$$

83

84 Terrestrial plant leaf wax *n*-alkane $\delta^2\text{H}$ values ($\delta^2\text{H}_{\text{terr}}$) have also been found to be linearly correlated to
85 the organisms source water $\delta^2\text{H}$ values, yet not in a 1:1 relationship (Sachse et al., 2012), indicating
86 additional influences on $\delta^2\text{H}_{\text{terr}}$ values. Recent greenhouse experiments and field studies have revealed
87 that in particular the evaporative ^2H enrichment of leaf water shapes $\delta^2\text{H}_{\text{terr}}$ values (Kahmen et al.,
88 2013a; Kahmen et al., 2013b). Soil water evaporation in the upper soil layers has been shown to be less
89 significant for $\delta^2\text{H}_{\text{terr}}$, as plants usually access the deeper, isotopically unenriched, soil layers (Dawson,
90 1993). As such, $\delta^2\text{H}_{\text{terr}}$ is affected mainly by the $\delta^2\text{H}$ value of plant source water (i.e. precipitation), the
91 biosynthetic fractionation and leaf water deuterium enrichment ($\Delta^2\text{H}_e$) (Eq. (2)).

92

$$(2) \delta^2\text{H}_{\text{terr}} = \delta^2\text{H}_{\text{precip}} + \Delta^2\text{H}_e + \epsilon_{\text{bio(terr)}}$$

93

94 Systematic differences in $\delta^2\text{H}_{\text{terr}}$ values have been observed for different plant types (especially
95 between grasses and trees) (Diefendorf et al., 2011; Kahmen et al., 2013b), possibly indicating
96 differences in either ϵ_{bio} (Sachse et al., 2012) or the fraction of leaf water used for lipid biosynthesis
97 (Kahmen et al., 2013b) or yet unidentified factors. As such, vegetation changes in sedimentary records
98 have been suggested to affect $\delta^2\text{H}_{\text{terr}}$ values and “vegetation corrections” have been proposed (Feakins,
99 2013).

100 Since evaporative ^2H enrichment of leaf water only affects terrestrial plants but not aquatic organisms,
101 changes in sedimentary $\delta^2\text{H}_{\text{terr}}$ (Sachse et al., 2006) can be seen as a record of variations in terrestrial
102 evaporative ^2H enrichment over time. Thus, by combining Eq. (1) and (2) under the assumption that ϵ_{bio}
103 of both aquatic and terrestrial organisms was constant on the temporal and spatial scales of sedimentary
104 integration, the difference between $\delta^2\text{H}_{\text{aq}}$ and $\delta^2\text{H}_{\text{terr}}$ values should mainly reflect the evaporative ^2H
105 enrichment of leaf water (Eq. (3)). Whenever referring to an ‘isotopic difference’ between two pools
106 (such as $\Delta^2\text{H}_e$) we employ the mathematical correct ‘epsilon’ formula to calculate differences between
107 two δ -values (Sessions and Hayes, 2005). For simplicity we use the following expression:

108

$$(3) \Delta^2\text{H}_e = \delta^2\text{H}_{\text{terr}} - \delta^2\text{H}_{\text{aq}}$$

109

110 Variants of this concept (Sachse et al., 2004) have been used to qualitatively interpret changes in
111 evapotranspiration through the isotopic difference between $\delta^2\text{H}_{\text{terr}}$ and $\delta^2\text{H}_{\text{aq}}$ (i.e. expressed as $\alpha_{\text{TA/wat}}$,
112 $\delta^2\text{H C}_{23}\text{--C}_{31}$ and $\epsilon_{\text{terr-aq}}$ (Jacob et al., 2007; Rach et al., 2014; Seki et al., 2011)). With recent progress in
113 understanding of the determinants of $\delta^2\text{H}_{\text{terr}}$ values and the existing mechanistic understanding of the
114 processes governing leaf water evaporative ^2H enrichment (Craig, 1965; Kahmen et al., 2011b; Sachse

115 et al., 2012), we propose a new framework – which we term the dual-biomarker (DUB) approach - to
116 extract quantitative hydrological information, namely changes in relative humidity (Δrh) from
117 sedimentary records. To illustrate the power of this approach with paleohydrological data, we combine
118 compound-specific hydrogen isotope measurements with plant physiological modeling on a previously
119 published Late Glacial record of δ^2H_{aq} and δ^2H_{terr} from sediments of Lake Meerfelder Maar (MFM),
120 Germany (Rach et al., 2014).

121

122 **2. Approach and Model**

123

124 The key assumptions of the DUB approach are that the difference between terrestrial and aquatic plant
125 derived *n*-alkane δ^2H values ($\epsilon_{terr-aq}$) equals evaporative Deuterium enrichment of leaf water (Kahmen
126 et al., 2013b; Rach et al., 2014) over the timescale of sediment integration (i.e. decades in our case) and
127 that $\delta^2H_{lake\ water}$ equals $\delta^2H_{mean\ annual\ precipitation}$, a condition fulfilled for small catchment lakes in temperate
128 environments without any major inflow. Also the temporal delay in transfer of terrestrial *n*-alkanes
129 from source organisms into lake sediment should be below the temporal resolution of the samples,
130 which is fulfilled for sites with a very small catchment area and steep terrain, such as maar lakes.
131 Furthermore we assume that the biosynthetic fractionation (ϵ_{bio}) is constant for terrestrial and aquatic
132 source organisms on temporal and spatial scales of sedimentary integration (Sachse et al., 2012). We
133 also assume, that palynological data represent lake catchment vegetation so that those can be used to
134 assess source organisms of aquatic and terrestrial *n*-alkanes (Rach et al., 2014; Schwark et al., 2002).
135 To assess the influence of vegetation changes on our reconstructions, we employ two different
136 vegetation corrections based on palynological data, for which we assume that the amount of *n*-alkanes
137 produced by these different plants is equal to the pollen produced by them.

138 These assumptions and additional data are needed to parameterize the model, therefore we emphasize
139 that a robust application of the DUB model requires a good understanding of the paleolake system and
140 its environment. As such, the DUB model should only be employed at a site which fulfills the
141 conditions presented above and where a number of additional, well constrained proxy data exist. As of
142 now, this limits the application of the DUB model to precipitation fed, small catchment (ideally maar
143 or crater) lakes in temperate regions.

144 δ^2H_{aq} in such systems can be regarded as a direct recorder of growing season average precipitation δ^2H
145 values and δ^2H_{terr} values largely reflect leaf water δ^2H values as has recently been demonstrated for
146 greenhouse and field grown plants (Kahmen et al., 2013a; Kahmen et al., 2013b). Leaf water in turn is
147 a function of the plant's source water and leaf water evaporative 2H enrichment. We argue that soil
148 water evaporation is negligible as recently suggested by several observational studies and a global
149 assessment (Jackson et al., 1996; Jasechko et al., 2013; Kahmen et al., 2013a) and that precipitation is
150 the ultimate water source of aquatic organisms and terrestrial plants. In terrestrial plants however, the
151 source water becomes more enriched in deuterium due to plant transpiration before it is used for lipid
152 biosynthesis. As such, the isotopic difference between δ^2H_{terr} and δ^2H_{aq} ($\epsilon_{terr-aq}$) can be attributed to
153 mean leaf water evaporative 2H enrichment (Δ^2H_e) (Sachse et al., 2004). Based on recent field and
154 greenhouse studies we further assume, that $\epsilon_{terr-aq}$ captures a growing season signal, probably biased

155 towards the earlier summer months in temperate climate zones as the majority of leaf waxes is
 156 produced during leaf development with suggested integrational periods between weeks (Kahmen et al.,
 157 2013b; Tipple et al., 2013) and several months (Sachse et al., 2015).

158
 159 The major variables controlling leaf water isotope enrichment are well understood and mechanistic
 160 models have been developed based on the Craig-Gordon evaporation model (Craig, 1965) that allow to
 161 accurately predict or reconstruct leaf water Δ^2H_e values based on environmental and physiological
 162 input variables (Barbour, 2007; Farquhar et al., 2007; Ferrio et al., 2009; Kahmen et al., 2011b) (Eq.
 163 (4))

$$(4) \quad \Delta^2H_e = \varepsilon_+ + \varepsilon_k + (\Delta^2H_{wv} - \varepsilon_k) \frac{e_a}{e_i}$$

164
 165 Δ^2H_e is determined by the equilibrium isotope fractionation between liquid and vapor (ε_+), the kinetic
 166 isotope fractionation during water vapor diffusion from the leaf intercellular air space to the
 167 atmosphere (ε_k), the 2H depletion of water vapor relative to source water (Δ^2H_{wv}), and the ratio of
 168 atmospheric vapor pressure and intracellular vapor pressure (e_a/e_i) and air temperature (T_{air}). In
 169 addition, leaf temperature (T_{leaf}), stomatal conductance (g_s) and boundary layer resistance (r_b) are
 170 essential secondary input variables for the prediction of e_i and ε_k , respectively. Reformulating Eq. (4)
 171 allows expressing e_a as a function of Craig-Cordon variables (Eq. (5)). Since the atmospheric vapor
 172 pressure (e_a) can also be calculated based on rh and saturation vapor pressure (e_{sat}) (Eq. (6)) we can
 173 merge Eq. (5) and (6) to calculate relative humidity (rh) and to estimate quantitative changes in rh
 174 (Δrh) (Eq. (7)).

175

$$(5) \quad e_a = \frac{e_i(\Delta^2H_e - \varepsilon_+ - \varepsilon_k)}{\Delta^2H_{wv} - \varepsilon_k}$$

176

$$(6) \quad rh = \frac{e_a \cdot 100\%}{e_{sat}}$$

177

$$(7) \quad \Delta rh = \frac{e_i(\Delta^2H_e - \varepsilon_+ - \varepsilon_k) \cdot 100\%}{e_{sat}(\Delta^2H_{wv} - \varepsilon_k)}$$

178

179 Equation (7) illustrates that Δrh can be inferred from a record of past changes in Δ^2H_e (i.e. a record of
 180 $\varepsilon_{terr-aq}$) if the additional variables e_{sat} , e_i , Δ^2H_{wv} , ε_+ and ε_k can be constrained. In the following we discuss
 181 the model parameterizations necessary to apply the DUB approach to estimate quantitative changes in
 182 rh from sedimentary records.

183

184 Saturation vapor pressure e_{sat} (Eq. (8)) as well as the equilibrium fractionation factor ε_+ (Eq. (9)) are a
 185 function of temperature (all given numbers and physically variable dependencies within the equations
 186 are transferred from the Péclet-modified Craig-Gordon model by Kahmen et al 2011b and the original
 187 leaf water enrichment model (Craig, 1965; Dongmann et al., 1974; Farquhar and Cernusak, 2005;

188 Farquhar and Lloyd, 1993)). The atmospheric pressure term (e_{atm}), which is also needed for calculation
 189 of e_{sat} , describes (mean annual) atmospheric pressure as a function of the elevation above sea level (0
 190 meters = 1013 hPa).

191

$$(8) e_{sat} = \frac{1.0007 + 3.46 \cdot e_{atm}[hPa]}{1000000} \cdot 6.1121 \cdot \exp\left(\frac{17.502 \cdot T_{air}[^{\circ}C]}{240.97 + T_{air}[^{\circ}C]}\right)$$

192

$$(9) \varepsilon_+ = \left[\exp\left(\frac{24.844 \cdot 1000}{(273.16 + T_{air}[^{\circ}C])^2} - \frac{76.248}{273.16 + T_{air}[^{\circ}C]} + 0.052612\right) - 1 \right] \cdot 1000$$

193

194 For accurate estimates of e_{sat} as well as ε_+ information on air temperature (T_{air}) during the growing
 195 season is thus required. Estimates of past T_{air} variability can be derived from paleotemperature proxy
 196 data to estimate e_{sat} and ε_+ (e.g. chironomids (Heiri et al., 2014; Heiri et al., 2007), MBT/CBT (Blaga et
 197 al., 2013)). In particular chironomid records, thought to represent spring and summer temperatures,
 198 provide an ideal proxy of past mean growing season temperatures in this respect (Heiri et al., 2007).
 199 Note that e_{sat} also depends on the atmospheric pressure (Eq. (8)), which can be estimated from
 200 elevation above sea level and is treated as a constant in the model. Leaf-internal vapor pressure e_i on
 201 the other hand is a function of leaf temperature (T_{leaf}). We assume for our calculations that T_{air} is a
 202 good estimate of a growing season average T_{leaf} and e_i can thus be calculated as:

203

$$(10) e_i = 6.13753 \cdot \exp\left(T_{air}[^{\circ}C] \cdot \frac{18.564 - \frac{T_{air}[^{\circ}C]}{254.4}}{T_{air}[^{\circ}C] + 255.57}\right)$$

204

205 We are aware that T_{leaf} can exceed air temperature in situations of extreme drought, when transpiration
 206 and evaporative cooling is reduced, or in bright and sunny conditions (Leuzinger and Korner, 2007;
 207 Scherrer et al., 2011). However, on cloudy days as well as on days with wind, T_{leaf} typically equals T_{air}
 208 (Jones, 2013). Given the spatial and temporal integration of leaves in sedimentary records (covering
 209 decadal to millennial timescales) it is thus unlikely that single drought events, where T_{leaf} would exceed
 210 T_{air} dominate the overall relationship between T_{leaf} and T_{air} . Recent studies also show that for
 211 temperatures between 15-20°C the T_{leaf} equals T_{air} on seasonal timescales (Kahmen et al., 2011b).

212 Another parameter affecting leaf water isotope enrichment is the 2H -depletion of water vapor relative
 213 to source water (Δ^2H_{wv}). In temperate climates liquid water and atmospheric water vapor are often in
 214 isotopic equilibrium, especially when longer (annual to decadal) timescales are investigated (Jacob and
 215 Sonntag, 1991). We therefore assume that Δ^2H_{wv} equals the equilibrium isotope fractionation between
 216 vapor and liquid ε_+ .

$$(11) \Delta^2H_{wv} = -\varepsilon_+$$

217

218

219

220 In the model, Δ^2H_{wv} can thus be replaced by $-\epsilon_+$ (Eq. (11)).

221 The kinetic isotope fractionation (ϵ_k) depends on the plant physiological variables stomatal
222 conductance (g_s) and boundary layer resistance (r_b) (Eq. (12)) (Kahmen et al., 2011b).

223

$$(12) \quad \epsilon_k = \frac{16.4 \cdot \frac{1}{g_s[\text{mol}/\text{m}^2/\text{s}]} + 10.9 \cdot r_b[\text{mol}/\text{m}^2/\text{s}]}{\frac{1}{g_s[\text{mol}/\text{m}^2/\text{s}]} + r_b[\text{mol}/\text{m}^2/\text{s}]}$$

224

225 No direct proxies exist to reconstruct these plant physiological variables from sedimentary records, but
226 paleovegetation data can be used to parameterize the model with biome-averaged values for g_s and r_b
227 that are inferred from modern plants (Klein, 2014). We note that these plant physiological variables
228 exert only minor control on the model outcome, expected to lie within the analytical error of δ^2H lipid
229 measurements (Kahmen et al., 2011b), see also discussion below.

230 The latest iterations of leaf water models also include a Péclet effect, which describes the ratio of
231 convective versus diffusional flow of water in the leaf (Eq. (4))(Kahmen et al., 2011b). However, we
232 did not include the Péclet effect in our calculations because we assume that variations in the Péclet
233 effect are minimal over time (Kahmen et al., 2009; Song et al., 2013) in particular for angiosperm
234 species.

235 When combining Eq. (9), (10), (11) and (12) with Eq. (7), we obtain a model for Δrh (Fig 1) that
236 requires only four major input variables: $\epsilon_{\text{terr-aq}}$, air temperature (T_{air}) as well as literature-derived values
237 for stomatal (g_s) and boundary layer conductance (r_b) and one constant parameter ('site altitude above
238 sea level' for atmospheric pressure (e_{atm})) to calculate Δrh :

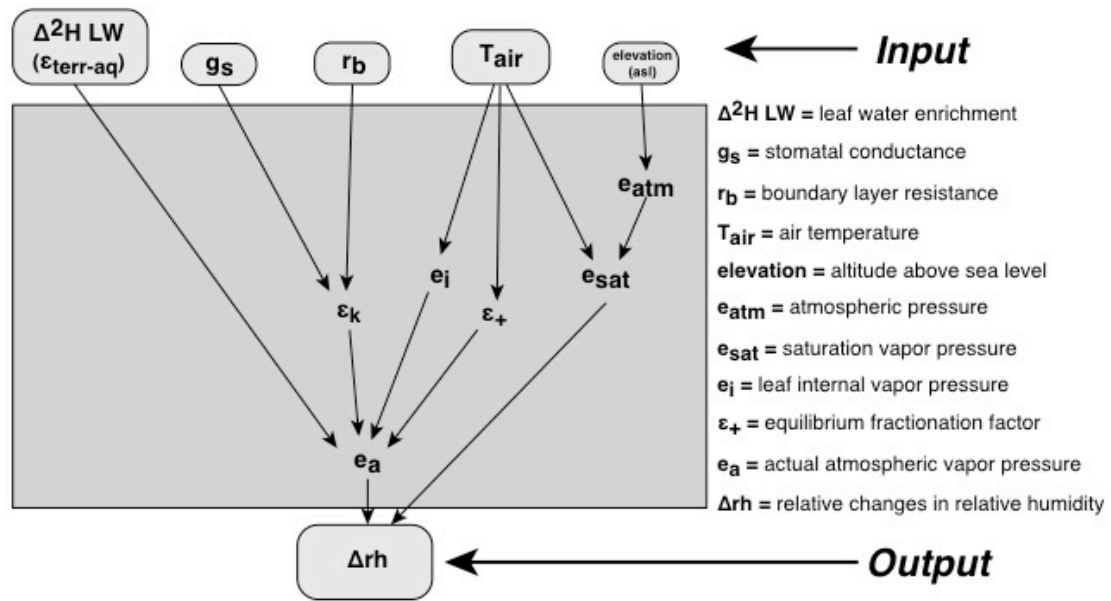
239

$$(13) \quad \Delta rh = e_i'(T_{\text{air}}) \cdot \left(\frac{\Delta^2 H_e}{-e_{\text{sat}}'(e_{\text{atm}}, T_{\text{air}})(\epsilon_+'(T_{\text{air}}) + \epsilon_k'(g_s, r_b))} + \frac{1}{e_{\text{sat}}'(e_{\text{atm}}, T_{\text{air}})} \right) \cdot 100\%$$

240

241 Since we use $\epsilon_{\text{terr-aq}}$ ($=\Delta^2H_e$) as an input variable, which is representative of leaf water isotope
242 enrichment above source water and not absolute δ^2H leaf water values, Eq. (13) predicts changes in rh
243 (Δrh) but not rh directly. In theory, Eq. (13) would also allow the calculation of rh values directly, if
244 absolute $\delta^2H_{\text{precip}}$ and $\delta^2H_{\text{leafwater}}$ was available. The current lack of experimentally determined
245 biosynthetic fractionation factors for the respective aquatic and terrestrial plants prevents this approach,
246 but future experimental research may result in robust estimates of ϵ_{bio} , potentially enabling the
247 reconstruction of absolute rh values (Zhang et al., 2009).

248



249

250

Fig. 1: Schematic overview showing the functional relationships between model variables of the DUB approach. Grey boxes on top mark the input parameters while the box size corresponds to the sensitivity of each variable on the result (small box → low influence on Δrh ; larger box → higher influence on Δrh)

251

252

253

254

255

3. Uncertainties and sensitivity tests

256

3.1 Uncertainties

257

258

259

The DUB approach contains different variables (Fig. 1) with specific error ranges which can be quantified. These quantifiable errors (i.e. analytical uncertainties during isotope measurement or paleotemperature determination as well as ranges of values) can be used to set up an error propagation function and finally to provide an error range for the results (e.g. Eq. 16, Appendix). However, additional to these quantifiable uncertainties there are some still some catchment related non-quantifiable uncertainties (see Table 1 – Appendix and chapter 2) which can increase the error of the results and therefore need to be taken in consideration before applying to a certain catchment/ record. These unquantifiable uncertainties can however be minimized through the selection of a particular, well characterized lacustrine archive, fulfilling the conditions we outlined under chapter 2.

260

261

262

263

264

265

266

267

268

3.2 Sensitivity tests

269

270

271

To evaluate the robustness of our DUB approach for predicting Δrh in the context of uncertainties, we tested the sensitivity of the model to uncertainties in the four key input variables T_{air} , $\epsilon_{\text{terr-aq}}$, g_s and r_b . In these sensitivity analyses we used a leaf water model, where all secondary variables (e_i , e_k , e_+ , e_{sat}) are coupled to the primary input variables T_{air} , T_{leaf} , g_s and r_b (Kahmen et al., 2011b). We performed this test under a range of dramatically different climatic and ecological settings reflected by the climate conditions of Lista (Norway), Koblenz (Germany), Genoa (Italy) and Perth (Australia) that differ in

272

273

274

275

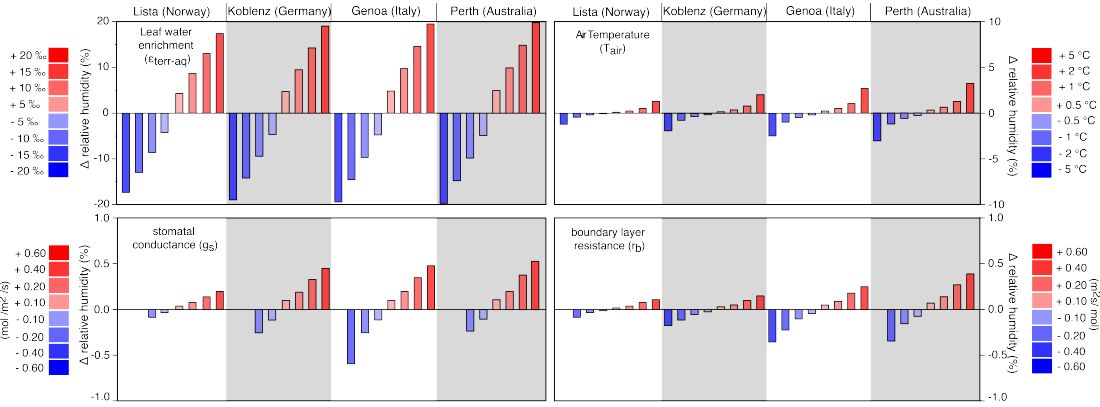
276

277 mean growing season temperatures and prevailing vegetation types. While the vegetation in Norway
278 and Australia is dominated by conifers and Mediterranean shrubland respectively, the prevailing
279 vegetation in Germany and Italy are broad leaf tree species. As baseline values for the sensitivity tests
280 we set T_{air} in the analyses to the growing season mean temperatures of each site, which was 9.4°C,
281 15°C, 17.2°C and 20.4°C for Lista, Koblenz, Genoa and Perth respectively (IAEA/WMO, 2006). Leaf
282 water evaporative enrichment $\epsilon_{\text{terr-aq}}$ ($\Delta^2\text{H}_e$) was set to 25‰ (Lista), 35‰ (Koblenz), 45‰ (Genoa) and
283 55‰ (Perth), which reflects average growing season leaf water enrichment values for the tested
284 environments (Kahmen et al., 2013a). Base line data for plant physiological variables were biome
285 typical estimates that we obtained from the literature (Jones, 2013; Klein, 2014): stomatal conductance
286 (g_s) for Lista and Koblenz was set to 0.25 mol/m²/s, while for Genoa and Perth the preset values were
287 0.45 and 0.35 mol/m²/s, respectively (Klein, 2014). Boundary layer resistance (r_b) for Lista and Perth
288 was set to 0.5 m²/mol, while for Koblenz and Genoa this variable was set to 1.0 m²/mol (Jones,
289 2013).

290 The temperature sensitivity tests were performed by increasing and decreasing the respective T_{air}
291 values for a location by 0.5°C, 1°C, 2°C and 5°C (encompassing reconstructed temperature variations
292 during the last major abrupt climate shift in western Europe – the Younger Dryas period with about 4-
293 6°C (Goslar et al., 1995; Heiri et al., 2007)). $\epsilon_{\text{terr-aq}}$ ($\Delta^2\text{H}_e$) values were varied by $\pm 5\%$, 10%, 15% and
294 20% for each location which corresponds to evaporative leaf water enrichment in the test areas (spring
295 months) (Kahmen et al., 2013a). Plant physiological variables (g_s and r_b) were varied by ± 0.1 , ± 0.2 ,
296 ± 0.4 and in maximum by ± 0.6 mol/m²/s and ± 0.6 m²/mol, respectively. These tested variations in
297 plant physiological variables cover the expected variation in g_s and r_b for the local vegetation at the
298 sites described in the sensitivity analysis.

299 The sensitivity analyses showed similar results for all four tested environments (Fig. 2). This suggests a
300 similar behavior of the model under very different climate and ecological conditions. The DUB model
301 is most sensitive to changes in $\epsilon_{\text{terr-aq}}$ (i.e. $\Delta^2\text{H}_e$) and T_{air} , while the plant physiological variables (g_s , r_b)
302 showed only minor effects on Δrh (Fig 2). Specifically, a change of $\pm 20\%$ in $\epsilon_{\text{terr-aq}}$ (i.e. $\Delta^2\text{H}_e$) resulted
303 in a change $\pm 20\%$ in Δrh . A $\pm 5^\circ\text{C}$ change in T_{air} resulted in a 3% change in Δrh . Varying g_s and r_b
304 within the specified limits caused only changes in Δrh of 0.01 to 0.5% (Fig. 2), suggesting low model
305 sensitivity to plant physiological variables. A sensitivity test with variations in atmospheric pressure
306 (e_{atm}) of $\pm 100\text{hPa}$ led to changes in Δrh of 0.05%. The difference in calculated Δrh for sites with low
307 (e.g. Lista) and high (e.g. Perth) growing season mean temperature were smaller than the regional
308 model sensitivity of the different input variables and are therefore negligible. Our sensitivity analyses
309 shows that the most critical variables for estimating changes in relative humidity with our model are
310 $\epsilon_{\text{terr-aq}}$ and T_{air} (Fig 2).

311



312

313

314

315

316

317

318

Fig. 2: Sensitivity analyses for major model input variables ($\epsilon_{\text{terr-aq}}$, T_{air} , g_s and r_b) on resulting Δrh values tested for four different climatic and ecological environments (Norway, Germany, Italy and Australia). Bars represent the effect on model output (Δrh) for each tested environment and its variation when the respective input variable will be varied by the marked value. Missing bars (i.e. for negative g_s and r_b) results from a bigger (negative) variation than the preset value (below 0).

319

4. Application: Reconstructing quantitative changes in Δrh during the Younger Dryas (YD) in Western Europe

320

321

322

323

324

325

326

327

328

329

330

331

332

333

334

335

In general, there are two approaches to validate a climate proxy. The most straight forward way is to test the proxy under modern hydroclimate conditions through variations in space or time and compare results with actual instrumental data, either along a modern climatological gradient or over the time period where instrumental data are available. The second possibility is the analysis of a longer time series during a period with otherwise known major changes in the parameter to be tested for. For testing the DUB model, the first approach is not feasible. While highly resolved (ideally annual laminated) lacustrine sediments from temperate Europe covering the instrumental period (roughly the last 150 years) exist, no major changes in relative humidity occurred during this time. Using only (non-laminated) core top sediments (i.e. only one data point integrating the last decade) would not allow for testing the performance of the DUB approach, which aims to reconstruct relative changes in relative humidity, not absolute data. Testing the DUB approach along a modern climatic gradient is also difficult, because we cannot assume that the source of aquatic biomarkers (in our case nC_{23}) is always the same aquatic macrophyte in different lakes and ecosystems (Sachse et al., 2004), i.e. it is unlikely to encounter enough lake systems where the sources of aquatic biomarkers are comparable and which cover a large enough aridity gradient.

336

337

338

339

340

341

342

343

Therefore we decided to employ the second approach, i.e. test the proxy during a period of known and significant changes in relative humidity, such as the YD cold period (Rach et al., 2014). The YD as the last major abrupt climatic shift in younger earths history (between 12680 years BP and 11600 years BP) was characterized by a significant temperature decrease of 4-6°C (Goslar et al., 1995; Heiri et al., 2007), a relocation of atmospheric circulation patterns (Brauer et al., 2008) as well as major hydrological changes (i.e. significantly drier conditions) and ecological variations (propagation of grass and reduction of tree vegetation) in western Europe (Brauer et al., 1999a; Litt and Stebich, 1999; Rach et al., 2014). The relocation of atmospheric circulations patterns during Northern Hemispheric cooling

344 led to drier conditions in western Europe. This forced changes in the regional vegetation composition
345 (Brauer et al., 1999a; Brauer et al., 2008; Rach et al., 2014). For this period a high resolution record of
346 changes in $\delta^2\text{H}_{\text{aq}}$ and $\delta^2\text{H}_{\text{terr}}$ from a lacustrine archive which fulfills the requirements outlined above
347 (i.e. precipitation fed, a very small catchment, available palynological and other climate proxy data
348 (Brauer et al., 1999a; Litt and Stebich, 1999)), Lake Meerfelder Maar (MFM) in western Germany,
349 exists. The presence of annual varves and a high temporal sampling resolution (decades) allow the
350 evaluation of the timing of climatic and ecosystem changes - an ideal setting to illustrate the power of
351 the DUB approach. A detailed description of the record and the available proxy data are given in Rach
352 et al. (2014). Briefly, the annually laminated sediments of MFM covering the YD period contain
353 abundant aquatic ($n\text{C}_{23}$) and higher terrestrial ($n\text{C}_{29}$) lipid biomarkers (n -alkanes) (Fig 3A). Based on
354 the pollen record, the $n\text{C}_{23}$ alkane can be related to the aquatic submerged plant *Potamogeton sp.* and
355 the $n\text{C}_{29}$ alkane to leaves originating from the terrestrial angiosperm trees *Betula sp.* and *Salix sp.* with
356 input from grasses (Brauer et al., 1999a; Diefendorf et al., 2011). For the DUB approach we use the
357 isotopic difference between $\delta^2\text{H}$ values of the $n\text{C}_{29}$ and of $n\text{C}_{23}$ alkanes ($\epsilon_{\text{terr-aq}}$) (Fig. 3B) as a measure
358 for leaf water ^2H enrichment ($\Delta^2\text{H}_e$).

359

360

361 **4.1 Model parameterization for the MFM application**

362 **4.1.1 Temperature**

363

364 Since no paleotemperature proxy data are directly available for MFM, we use a high-resolution
365 chironomid based temperature reconstruction from a nearby location, lake Hijkermeer in the
366 Netherlands (Fig 3C), ca. 300 km N of MFM (see the Appendix). The Hijkermeer record is interpreted
367 as a record of mean July temperatures for Western Europe with an mean error of about 1.59°C (Heiri et
368 al., 2007). Since leaf wax synthesis occurs most likely during the early part of the growing season
369 (spring and summer) (Kahmen et al., 2011a; Sachse et al., 2015; Tipple et al., 2013), the Hijkermeer
370 record might slightly overestimate spring temperatures. However, when reconstructing Δrh during the
371 Younger Dryas, it is important that paleotemperature data capture the changes in temperature before
372 and during that period, rather than absolute temperatures.

373

374 **4.1.2 Plant physiological parameters**

375

376 We estimated plant physiological variables (g_s and r_b) based on literature data from the prevalent
377 catchment vegetation inferred from available MFM pollen records (Brauer et al., 1999a; Litt and
378 Stebich, 1999). These suggest that *Betula sp.* and *Salix sp.* were the dominant $n\text{C}_{29}$ producing taxa but
379 that grasses became more abundant during the YD (Brauer et al., 1999a; Litt and Stebich, 1999).
380 Reported g_s values for these species growing under humid to arid conditions today range from 0.1 to
381 0.5 mol/m²/s and boundary layer resistance (r_b) values from 0.95 to 1.05 mol/m²/s (Klein, 2014;
382 Schulze, 1982, 1986; Turner, 1984). As input variables for our modified model we therefore used mean
383 values, i.e. 0.3 mol/m²/s for g_s and 1.0 mol/m²/s for r_b . We used the variance of ± 0.2 mol/m²/s for g_s

384 and $\pm 0.1 \text{ mol/m}^2/\text{s}$ for r_b to calculate the error range of Δrh . We note the low sensitivity of the DUB
385 model outcome to variability in these variables (see Fig. 2, Appendix), as such that Δrh changes of less
386 than 0.1% result from varying g_s by $0.4 \text{ mol/m}^2/\text{s}$ or r_b by $0.1 \text{ mol/m}^2/\text{s}$ (Fig. 2).

387 **4.2 Estimation of uncertainty**

388

389 The estimation of uncertainty for Δrh is based on a linear error propagation (Eq. (16) - in the
390 Appendix) using specific error ranges for the individual input variables. For each input variable we
391 used their individual reported or estimated error (i.e. for chironomid interfered temperature
392 reconstruction: $\pm 1.5^\circ\text{C}$), for $\epsilon_{\text{terr-aq}}$ the analytical uncertainty (standard deviation) of the respective
393 biomarker $\delta^2\text{H}$ measurements and for g_s and r_b the observed range of plant physiological parameters
394 between different species (g_s : $0.1\text{-}0.5 \text{ mol/m}^2/\text{s}$, r_b : $0.95\text{-}1.05 \text{ m}^2/\text{s/mol}$). The resulting average error for
395 Δrh estimation during the investigated interval is 3.4% (see above and in the Appendix).

396

397

398 **4.3 Model results for the YD period at MFM**

399

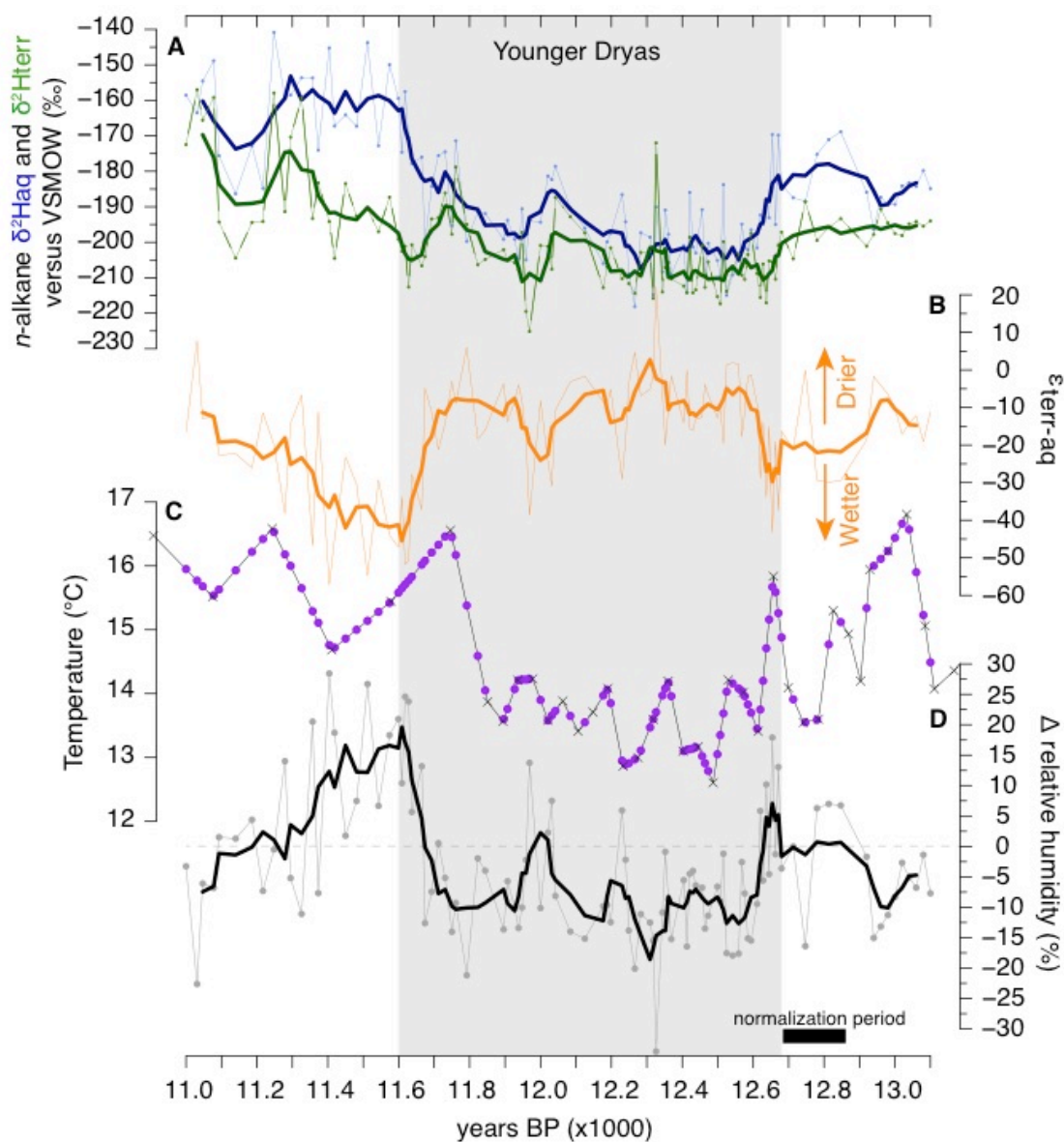
400 Applying the DUB approach to the Late Glacial MFM record we can for the first time estimate the
401 magnitude by which rh changed during a distinct period of abrupt climatic change in the past. Our
402 quantification revealed substantial changes in relative humidity (Δrh) on the order of 30% (Fig 3D)
403 during the Late Glacial period, some of which occurred on multi-decadal timescales. To better illustrate
404 these changes we normalized our results to the mean of the period between 12.847 – 12680 BP (mean
405 Allerød) (Fig 3D), which is thought to have been warmer and moister than the Younger Dryas (Hoek,
406 2009).

407 In particular, at the onset of the YD at 12.680 years BP, Δrh decreased by 13% \pm 3.4% over 112 years
408 compared to mean Allerød level (Fig. 3D). During the YD (from 12.680-11.600 years BP) Δrh values
409 were on average 5% \pm 3.4% lower compared to the mean Allerød level. Furthermore in our high-
410 resolution dataset we observe a division of the YD into two distinct phases: the first part of the YD
411 (12.610-12.360 years BP) was characterized by low but relatively constant Δrh (variability between -
412 8% and -13% and a mean of -10%, compared to Allerød), whereas the variability in Δrh increases after
413 12360 years BP and ranges between -19% and +2% and a mean of -8% compared to Allerød mean
414 values (Fig. 3D). Towards the termination of the YD we reconstructed a strong increase in Δrh (up to
415 +20% above the Allerød level) over only 80 years. This increase started about 100 years before the YD
416 – Holocene transition at 11.600 BP (Fig. 3D), indicating that hydrological changes lead major
417 ecosystem changes, which formed the basis for the definition of the YD-Holocene boundary (Brauer et
418 al., 1999a; Brauer et al., 1999b). The onset of the Holocene was characterized by substantial variability
419 in Δrh , with a strong increase followed by a decrease to mean Allerød levels 150 years after the
420 transition. The reconstructed magnitude of changes, i.e. a ca. 9% reduction in rh during the YD
421 constitutes a shift from an oceanic to a dry summer climate, comparable to the difference in mean
422 annual rh between Central and Southern Europe today (Center for Sustainability and the Global
423 Environment (SAGE), 2002; New et al., 1999). The overall temporal pattern of reconstructed Δrh

424 changes is in good agreement with proxy data from western Europe (Bakke et al., 2009; Brauer et al.,
 425 1999a; Brauer et al., 2008; Goslar et al., 1993), which indicate a shift to drier conditions due to a
 426 southward displacement of the westerly wind system channelling dry, polar air into Western Europe
 427 (Brauer et al., 2008; Rach et al., 2014).

428 Our approach reveals for the first time that substantial changes in rh of up to 20% can take place over
 429 very short time scales, i.e. several decades, leading to substantial changes in terrestrial ecosystems.
 430 While other proxy data reveal qualitative trends in aridification, our approach can be used to identify
 431 hydrological thresholds. Applied to high-resolution records, such as annually laminated lake sediments,
 432 the DUB approach can even be used to derive rates of hydrological changes and compare those with
 433 associated ecological changes (i.e. pollen records).

434



435

436 **Fig. 3:** (A) $\delta^2\text{H}$ values of aquatic plants ($\delta^2\text{H}_{\text{aq}}$, blue line) and higher terrestrial plants ($\delta^2\text{H}_{\text{terr}}$, green line
 437 (Rach et al., 2014). (B) Terrestrial evapotranspiration ($\epsilon_{\text{terr-aq}}$, orange line) during the Younger Dryas at
 438 MFM (Rach et al., 2014). (C) Original chironomid based temperature reconstruction from Hijkermeer

439 (NL) (Heiri et al., 2007) (black line with X as data points) and interpolated temperature data for DUB
440 approach (purple dots). **(D)** Variability of Δrh during the YD cold period at MFM. The data are
441 normalized to mean Allerød level (12.847 – 12.680 years BP). The bold line marks the moving
442 average.

443

444 **4.4 The effect of vegetation change on $\epsilon_{terr-aq}$ and the estimation of Δrh**

445

446 Numerous studies have established that vegetation changes can also affect the sedimentary leaf wax
447 δ^2H record, since significant differences in the net or apparent fractionation (ϵ_{app}) between source water
448 and lipid δ^2H values exist among different plant types, in particular between monocot and dicot (all
449 grasses) plants (Kahmen et al., 2013b; Tipple et al., 2013). Since the YD period at MFM was
450 characterized by an increased amount of grasses, we tested, how vegetation changes may affect Δrh
451 reconstructions through the DUB approach. For this we have developed two approaches to “correct”
452 δ^2H_{terr} values, based on either a constant offset between monocot and dicot ϵ_{app} (Sachse et al., 2012) or
453 a lower sensitivity of grass derived leaf wax δ^2H values to leaf water isotope enrichment (Kahmen et
454 al., 2013b). Both approaches assume that palynological reconstructions are representative of leaf wax
455 producing plants and that both monocots and dicots produce similar quantities of *n*-alkanes.

456 We used available palynological data to quantify the relative distribution of major tree vegetation
457 (*Betula*, *Salix*) and grasses over the investigated period (Fig. 4B), expressed as the fraction of trees and
458 grasses, f_{trees} and f_{grass} , assuming that leaf waxes and pollen share a similar transport pathway in this
459 small, constrained crater catchment.

460

461 **4.4.1 Correction - case 1 – constant difference in ϵ_{app} between monocots and dicots**

462

463 The first vegetation correction for reconstructed leaf water enrichment ($\epsilon_{terr-aq}^*$) is based on the
464 assumption of a constant offset in biosynthetic isotope fractionation (ϵ_{bio}) between trees and grasses.
465 Observational evidence shows that leaf wax lipid δ^2H values (δ^2H_{terr}) from C3 monocots are on average
466 34‰ more negative than from C3 dicots (non-grasses) when growing at the same site (Sachse et al.,
467 2012). This value is based on an observed mean difference between apparent isotope fractionation (i.e.
468 the isotopic difference between source water and leaf wax *n*-alkanes, ϵ_{app}) values of C3 dicots (-111‰)
469 and C3 monocots (-141‰) within a global dataset (Sachse et al., 2012).

470 The difference between monocot and dicot *n*-alkane δ^2H could potentially affect our modeled Δrh
471 values, especially since an 23% increase in grass abundance in the MFM catchment during the YD has
472 been suggested by pollen studies (Brauer et al., 1999a; Litt and Stebich, 1999). The causes for these
473 differences in ϵ_{app} have been hypothesized to be due to species-specific differences in biosynthetic
474 fractionation (Sachse et al., 2012) or temporal differences in leaf wax synthesis during the growing
475 season (Tipple et al., 2013). Both scenarios would result in a more or less constant isotopic offset
476 between monocots and dicots growing under the same climatic conditions.

477 Assuming a mean isotopic difference of -34‰ between trees and grasses (Sachse et al., 2012), we
478 calculated a vegetation weighted correction value ($-34 * f_{grass}$) for each data point. This value is then

479 subtracted from $\epsilon_{terr-aq}$, and results in the vegetation corrected $\epsilon_{terr-aq}^*$ value (Eq. (14)). Similar
480 approaches for a pollen based vegetation reconstruction have been recently proposed and applied
481 (Feakins, 2013; Wang et al., 2013).

482

$$(14) \quad \epsilon_{terr-aq}^* = \epsilon_{terr-aq} - (-34 \cdot f_{grass})$$

483

484 **4.4.2 Correction - case 2: different sensitivity to leaf water isotope enrichment in dicot vs.** 485 **monocot leaf wax $\delta^2\text{H}$ values**

486

487 The second vegetation correction ($\epsilon_{terr-aq}^{**}$) is based on the assumption that the isotopic difference
488 between monocot and dicot leaf wax n -alkanes is not constant, but dependent on environmental
489 conditions (Kahmen et al., 2013b). Previous greenhouse studies imply that the difference in ϵ_{app}
490 between dicots and monocots is variable depending with a change in humidity conditions (Kahmen et
491 al., 2013b). In a high humidity climate chamber treatment (80% rh) monocots and dicots showed
492 similar values for ϵ_{app} (-220‰ and -214‰ respectively) whereas in a low humidity treatment ϵ_{app} for
493 monocots was substantially lower compared to dicots (-205‰ and -125‰ respectively) (Kahmen et al.,
494 2013b), a finding that is in disagreement with the two hypotheses proposed above. Rather, the latter
495 study hypothesized that grasses use a mixture of enriched leaf water and unenriched xylem water for
496 lipid synthesis (Kahmen et al., 2013b). This hypothesis would imply that leaf wax n -alkane $\delta^2\text{H}$ values
497 of monocots do not record the full magnitude of the evaporative leaf water enrichment signal, but only
498 a fraction (Sachse et al., 2009). A recent greenhouse study on grass derived n -alkane $\delta^2\text{H}$ values of a
499 broad spectrum of C3 and C4 grasses support this idea (Gamarra et al., 2016). Gamarra et al. suggest
500 that the differences between n -alkane $\delta^2\text{H}$ values from grasses and n -alkane $\delta^2\text{H}$ values from
501 dicotyledonous plants are caused by an incomplete transfer of leafwater $\Delta^2\text{H}$ to the n -alkanes. As such,
502 a sedimentary record of n -alkanes derived partly from grasses would also underestimate mean
503 ecosystem leaf water enrichment. Under dry conditions this fraction was estimated to be ca. 18% for
504 C3 grasses, based on one grass species (Wheat) studied (Kahmen et al., 2013b). The data from
505 Gamarra et al. show that for C3 grasses only 38 – 61% of the leaf water evaporative ^2H -enrichment
506 signal (depending on the species) was transferred to leaf wax n -alkane $\delta^2\text{H}$ values. To work with a
507 conservative value and not to overestimate a potential leaf water enrichment signal in grass derived n -
508 alkane $\delta^2\text{H}$ values we decided to use the data from Kahmen et al. (2013) for the wheat C3 grass. As
509 such our correction approach would rather underestimate changes in relative humidity and represents as
510 such the lower limit of reconstructed changes.

511 Under the assumption of different sensitivities to leaf water isotope enrichment of n -alkane $\delta^2\text{H}$ values
512 in monocot and dicot plants (Kahmen et al., 2013b) we developed a correction for $\epsilon_{terr-aq}$ based on the
513 experimentally determined mixing ratio between leaf water and unenriched xylem water in wheat, a C3
514 grass (Kahmen et al., 2013b), essentially by weighing the fraction of grass cover with a factor of 0.18:
515 (Fig. 4B) (Eq. (15)).

516

$$(15) \quad \epsilon_{terr-aq}^{**} = (f_{trees} \cdot 1 + f_{grass} \cdot 0.18) \cdot \epsilon_{terr-aq}$$

517

518 **4.5 Comparison of results from uncorrected ($\epsilon_{\text{terr-aq}}$) and corrected ($\epsilon_{\text{terr-aq}}^*$, $\epsilon_{\text{terr-aq}}^{**}$) values**

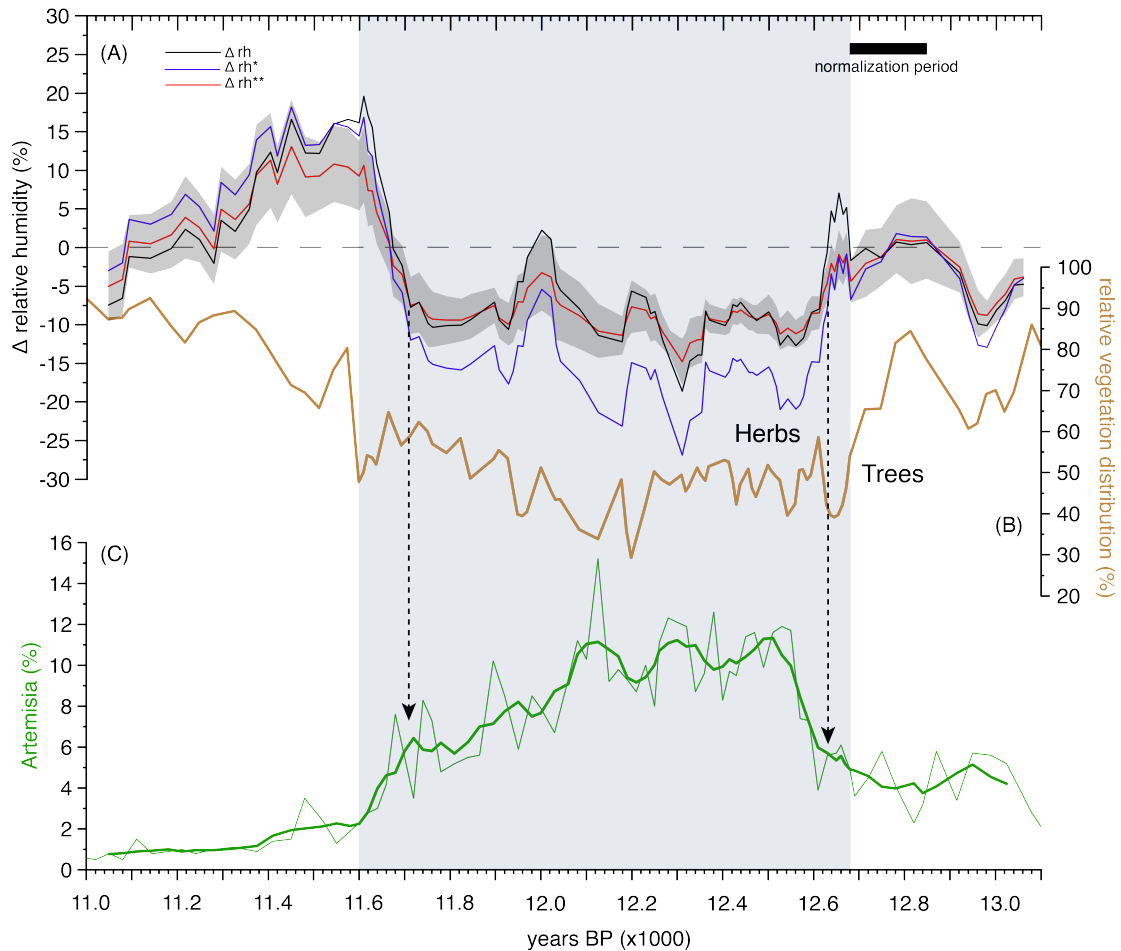
519

520 Results from the raw (Δrh) and both vegetation corrected scenarios (Δrh^* and Δrh^{**}) are within the
521 calculated error range of 3.4% of Δrh (Fig. 4A) during the Allerød and the Early Holocene, but diverge
522 by up to 10% during the YD, when C3 grass vegetation was estimated to have increased from 28% to
523 52% in the catchment of MFM (Fig. 4B). Vegetation corrected results (case 1 Fig. 4A) showed on
524 average a 7% stronger decrease for Δrh^* and only a 2% stronger decrease for Δrh^{**} compared to
525 uncorrected results. As such Δrh^{**} values (case 2) are within the error range of uncorrected Δrh during
526 the entire record.

527 Interestingly, both correction approaches, but in particular case 2, place the relatively large variability
528 in uncorrected Δrh at the onset and the termination of the YD, where abrupt vegetation changes
529 occurred. For example, uncorrected Δrh changes were predicted to be up to 35% during the termination
530 of the YD, corresponding to the modern gradient between western Europe and the semi-desert areas in
531 northern Africa (Center for Sustainability and the Global Environment (SAGE), 2002). Vegetation
532 corrected Δrh^{**} values were on the order of 20%, seemingly more reasonably representing local Late
533 Glacial changes (Fig. 4A).

534 Our analysis shows that vegetation changes have the potential to affect the DUB approach estimates,
535 but a lack of mechanistic understanding of the causes of the differences in $\delta^2\text{H}_{\text{terr}}$ between tree and
536 grass vegetation (Sachse et al., 2012) makes an assessment of the validity of either (or any) correction
537 approach difficult. Tentatively, the lower variability in Δrh^{**} within the YD as well as the less
538 pronounced shift in particular at the onset and termination of the YD (Fig. 4A) provides a more
539 realistic scenario. But as of now, we regard the differences in predictions as the error of quantitative
540 predictions from the DUB approach. This uncertainty is larger during periods characterized by
541 vegetation changes and in our case maximum differences in prediction of Δrh between the Allerød and
542 the YD are on the order of 11% (mean Allerød vs mean YD difference between Δrh and Δrh^*).

543

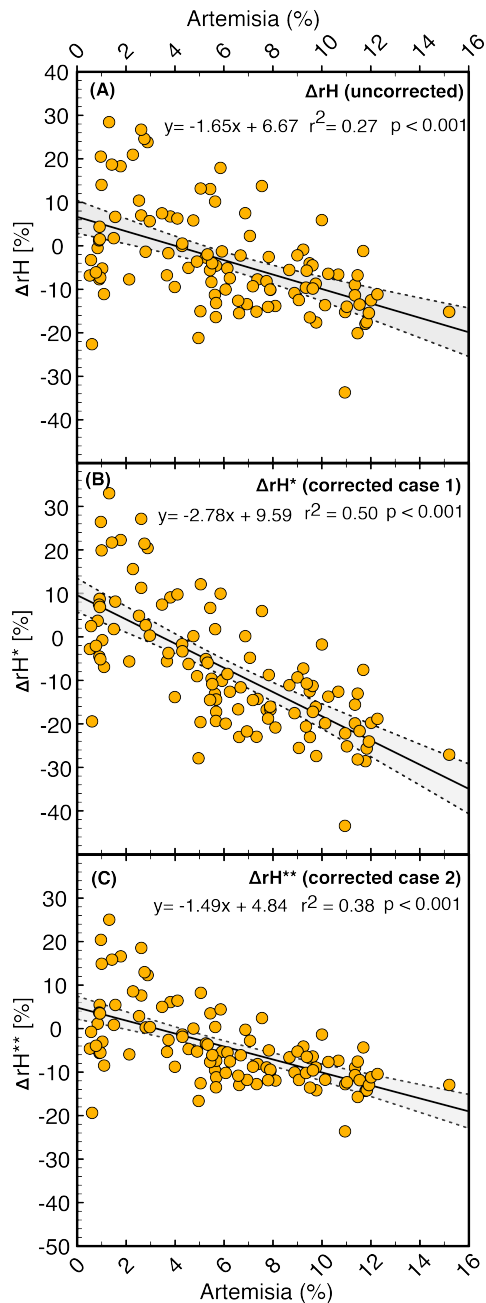


544
 545 **Fig. 4:** (A) Reconstructed Δrh variability during the YD period (light grey shaded), without vegetation
 546 correction (**black line, Δrh**) with vegetation correction assuming a constant offset between C3 dicots
 547 and C3 monocots (**blue line, Δrh^***), with vegetation correction assuming different leaf water
 548 sensitivities among grasses and trees (**red line, Δrh^{**}**). The shaded area marks the error range for
 549 Δrh^{**} . (B) relative distribution of trees and grasses in the catchment of MFM during the YD from
 550 pollen studies (Brauer et al., 1999a; Litt and Stebich, 1999). (C) Occurrence of *Artemisia* pollen in the
 551 catchment of MFM during YD (Brauer et al., 1999a; Litt and Stebich, 1999). Arrows highlight the
 552 contemporaneous major changes in Δrh and *Artemisia*.

553
 554 **4.6 Comparison of reconstructed Δrh with other proxy data**

555
 556 We can further demonstrate the validity of our approach by direct comparison to other hydroclimate
 557 proxies from the MFM record. For example, a classical palynological marker for more arid conditions
 558 is *Artemisia* pollen (D'Andrea et al., 2003). In the MFM catchment a prominent increase in the
 559 occurrence of *Artemisia* has been used to infer drier conditions during the YD (Fig. 4C) (Brauer et al.,
 560 1999a; Bremer and Humphries, 1993; D'Andrea et al., 2003; Litt and Stebich, 1999). When comparing
 561 the abundance of *Artemisia* pollen % (note that the *Artemisia* abundance data are not part of the
 562 vegetation corrections discussed above) to the DUB Δrh record, we observed striking similarities over
 563 the whole of the study period (Fig. 4A,C). Inferred wetter conditions during the second phase of the

564 YD, or centennial scale excursions to higher Δrh (such as between 12280 and 12170 years BP) go in
 565 line with lower *Artemisia* pollen abundance after 12.100 BP. In fact, both independent datasets show an
 566 inverse, statistically significant relationship ($p < 0.001$) (Fig. 5A-C), with high *Artemisia* pollen
 567 abundance during periods of low Δrh values (Fig. 4A,C). The correlation between Δrh and *Artemisia* is
 568 higher for vegetation corrected Δrh^* and Δrh^{**} (Fig. 5B,C) than uncorrected Δrh and in particular for
 569 Δrh^{**} the variance of the dataset is greatly reduced (Fig. 5C), providing support for the hypothesis that
 570 vegetation changes could have affected the record.
 571



572
 573 **Fig. 5:** Correlation plots of normalized reconstructed Δrh vs. *Artemisia* population. (A) uncorrected Δrh
 574 values vs. *Artemisia*. (B) Vegetation corrected Δrh values (Δrh^*) vs *Artemisia*. (C) Vegetation
 575 corrected Δrh values (Δrh^{**}) vs *Artemisia*.
 576

577 **5. Conclusions**

578

579 We present a novel approach for quantifying paleohydrological changes (i.e. changes in relative
580 humidity) combining sedimentary lipid biomarker $\delta^2\text{H}$ values from aquatic and terrestrial lipids with
581 mechanistic leaf water isotope modeling. This dual-biomarker approach (DUB) relies on the
582 observation that aquatic and terrestrial organisms within the catchment of small lakes from temperate
583 climate zones use distinct water sources, namely lake (i.e. precipitation) and ^2H -enriched leaf water as
584 a source for their organic hydrogen. By taking advantage of the mechanistic understanding of and
585 available models on leaf water isotope enrichment in terrestrial plants, we show it is possible to extract
586 quantitative information about changes in relative humidity from sedimentary records.

587 Parameterizing and applying the DUB model to a lacustrine lipid biomarker $\delta^2\text{H}$ record from western
588 Europe, we find strong and abrupt changes in rh at the onset and the termination of the YD occurring
589 within the lifetime of a human generation. Specifically, our approach showed that shifts in rh of up to
590 13% +/- 3.4% occurred within only 112 years. This dramatic change corresponds to shifts in average
591 biome rh from oceanic to dry summer climates. Our quantification showed that dry conditions
592 prevailed during the Younger Dryas period with rh being between 8 and 15% lower on average
593 compared to the Allerød, depending on how the possible effect of vegetation changes is accounted for.
594 The pattern but also the magnitude of our rh reconstruction agrees well with other proxy data, such as
595 the increase in the abundance of specific taxa adapted to dry conditions (e.g. *Artemisia*) during that
596 time period.

597 Our analyses shows that the DUB approach is capable of quantifying past hydrological changes in
598 temperate environments, when additional proxy data, especially on vegetation distribution and
599 paleotemperature exist. We suggest that this approach can be particularly valuable in the future for the
600 validation of climate models and to better understand uncertainties in predictions of future hydrological
601 change under global warming. However, we stress that the DUB approach relies on a number of
602 assumptions and is currently limited by our incomplete understanding of processes affecting the
603 transport and deposition of in particular terrestrial biomarkers from their source to the sedimentary
604 sink. To minimize the arising uncertainties, this approach should only be applied to small catchment
605 lake systems which are fed by precipitation in temperate climate zones, when biomarker sources can be
606 constrained by paleovegetation data (such as palynological records). It is particularly crucial to
607 constrain the aquatic biomarker source, but in principle any aquatic lipid biomarker (macrophyte, algal)
608 could be employed. Our reconstruction provides reasonable values of rh changes during the YD cold
609 period, which are in agreement with ecosystem changes in the region. As such, the present approach
610 provides a first step towards quantitative paleohydrological reconstructions.

611

612

613

614

615

616

617 **Appendix**

618

619 **Error propagation**

620

621 The uncertainty estimation (Δf , Eq. (16)) for the reconstructed Δrh variability is based on a linear error
622 propagation, which is the most conservative method for error estimations. This Method does not
623 require the same kind of the considered errors and provides therefore the possibility to combine
624 different kinds of errors with their specific ranges (i.e. measuring error, counting error, etc.). The
625 individual error ranges of the independent variables in our approach arise from different sources such
626 as analytical errors (chironomid interfered temperature reconstruction: $\pm 1.5^\circ\text{C}$), observed variations of
627 plant physiological parameters between different species (stomatal conductance: $0.1\text{-}0.5 \text{ mol/m}^2/\text{s}$,
628 boundary layer resistance: $0.95\text{-}1.05 \text{ m}^2/\text{s/mol}$) and standard deviation of $\delta^2\text{H}$ measurements of
629 terrestrial and aquatic *n*-alkanes.

630 The specific uncertainty for $\varepsilon_{\text{terr-aq}}^{**}$ was preliminary determined by a separate error propagation using
631 the (analytical) standard deviation of the triplicate measurements of the sedimentary *n*-alkane $\delta^2\text{H}$
632 values as well as the plant derived *n*-alkane $\delta^2\text{H}$ measurements by Kahmen et al 2013. The results of
633 these separate error estimation were integrated into the general error estimation of Δrh^{**} .

634 In contrast to the linear error propagation a less conservative method (Gaussian error propagation)
635 requires a similarity of the errors, i.e. all errors are measurement or counting errors, which is not the
636 case in this study. The mean error when using the Gaussian method is however only 3.2% and therefore
637 only 0.2% smaller than the calculated error using the linear propagation.

638

639

$$(16) \quad \Delta f = \left| \frac{\partial rh}{\partial \varepsilon_{\text{terr-aq}}} \right| \cdot \Delta \varepsilon_{\text{terr-aq}}^{**} + \left| \frac{\partial rh}{\partial r_b} \right| \cdot \Delta r_b + \left| \frac{\partial rh}{\partial g_s} \right| \cdot \Delta g_s + \left| \frac{\partial rh}{\partial T_{\text{air}}} \right| \cdot \Delta T_{\text{air}}$$

640

641

642 **Temperature data**

643

644 The temperature data used for the DUB model parameterization of the MFM case were taken from ref.
645 35 and constitute reconstructed summer temperatures based on chironomid analyses from Hijkermeer
646 (NL) (Heiri et al. (2007)), which, to our knowledge, constitutes the closest lateglacial paleotemperature
647 record to the MFM site (distance 311km). However, the dataset of the Hijkermeer consists only of 37
648 data-points between 13.000 BP and 11.000 BP with a temporal resolution varying between 26 to 167
649 years /sample. Therefore, we determined a new equidistant time-series for the temperature data, fitting
650 data-volume and temporal resolution of our $\Delta^2\text{H}_c$ record from MFM (106 data-points with an 8 to 33
651 year-resolution). For calculating the equidistant time series we were using method “interpl” with the
652 specification “linear” in MATLAB (version R2010b).

653

654

655
656

Table 1: Major model assumptions

assumption	explanation
$\delta^2\text{H}_{\text{lake water}} = \delta^2\text{H}_{\text{mean annual precipitation}}$	Stable hydrogen isotope composition of lake water equals mean annual stable hydrogen isotope compositions of precipitation (source water), as observed for small catchment lakes in temperate environments (Moschen et al., 2005)
$\epsilon_{\text{terr-aq}} = \text{leaf water evaporative } ^2\text{H enrichment}$	Difference between terrestrial and aquatic plant derived <i>n</i> -alkane $\delta^2\text{H}$ values equals evaporative Deuterium enrichment of leaf water (Kahmen et al., 2013b; Rach et al., 2014)
$\epsilon_{\text{bio}} = \text{constant}$	Biosynthetic fractionation is constant for aquatic as well as terrestrial source organisms on temporal and spatial scales of sedimentary integration (Sachse et al., 2012)
no significant delay (i.e. below sample resolution, i.e. decades) of terrestrial <i>n</i> -alkanes transfer from source organisms into lake sediment	Due to the very small catchment of MFM with steep and wind sheltered crater walls we can assume an almost instantaneous transfer of <i>n</i> -alkanes and pollen from source organisms to lake sediment. Likely autumn leaf litter is the main <i>n</i> -alkane source to the sediment. This is supported by the similar sample to sample (i.e. decadal) variability in the lipid $\delta^2\text{H}$ values. If, for example, terrestrial leaf wax <i>n</i> -alkanes would have a substantially longer residence time in the soils before being transported into the lake, then the decadal variability should be much smaller, as the soil would already deliver a more integrated signal into the lake
$\epsilon_{\text{atm}} = \text{constant}$	The atmospheric pressure is inferred from the altitude above sea level (0 meters = 1013 hPa), which remained unchanged. Short term weather related fluctuations (on the order of 100hPa) do not affect the model outcome (see text).
$T_{\text{leaf}} = T_{\text{air}}$	Leaf temperature equals air temperature on the timescale of sediment integration (decades) (Kahmen et al., 2011b)
$\Delta^2\text{H}_{\text{wv}} = -\epsilon_+$	atmospheric water vapor equals equilibrium isotope fractionation between vapor and liquid, as often observed for long-term (several years) time series in temperate climates (Jacob and Sonntag, 1991)
no significant influence by Péclet effect	Variations in the Péclet effect are minimal over time in particular for angiosperm species (Kahmen et al., 2009; Song et al., 2013)
amount of produced <i>n</i> -alkanes from monocots and dicots are almost equal	Both of our vegetation correction approaches assume that palynological reconstructions are representative of leaf wax producing plants and that both monocots and dicots produce similar quantities of <i>n</i> -alkanes.

657
658
659
660
661
662

663 **Vegetation data**

664 Information about Lateglacial vegetation-cover in the catchment area of MFM is based on
665 palynological analyses (Brauer et al. (1999), Litt & Stebich (1999)). We used Pollen percent data also
666 for determining the vegetation distribution between trees and grasses for each datapoint. For using
667 these vegetation data in our model it was necessary to determine an equidistant time-series according to
668 age model of our Δ^2H_e values. For calculating these time series we used also method “interpl” with the
669 specification “linear” in MATLAB (version R2010b).

670

671 **Author contributions**

672 Oliver Rach conducted model modifications, calculations and wrote the paper. Ansgar Kahmen
673 provided the basic leaf water enrichment model and was responsible for plant physiological part and
674 contributed in writing the paper. Achim Brauer was responsible for lake coring, provided the
675 chronology and stratigraphy for Younger Dryas hydrological reconstruction and wrote the paper. Dirk
676 Sachse conceived the research, acquired financial support and wrote the paper.

677 **Competing financial interests**

678 The authors declare no competing financial interests.

679

680 **Acknowledgements**

681

682 This work was supported by a DFG Emmy-Noether grant (SA1889/1-1) and an ERC Consolidator
683 Grant (No. 647035 *STEEP*clim) to D.S. It is a contribution to the INTIMATE project, which was
684 financially supported as EU COST Action ES0907 and to the Helmholtz Association (HGF) Climate
685 Initiative REKLIM Topic 8, Rapid climate change derived from proxy data, and has used infrastructure
686 of the HGF TERENO program.

687

688 **References**

- 689 Aichner, B., Herzschuh, U., Wilkes, H., Vieth, A. and Böhner, J. (2010) δD values of n-alkanes in
690 Tibetan lake sediments and aquatic macrophytes - A surface sediment study and application to a 16 ka
691 record from Lake Koucha. *Organic Geochemistry* 41, 779-790.
- 692 Alley, R.B. (2000) Ice-core evidence of abrupt climate changes. *Proc. Natl. Acad. Sci. U. S. A.* 97,
693 1331-1334.
- 694 Alley, R.B. and Cuffey, K.M. (2001) Oxygen- and Hydrogen-Isotopic Ratios of Water in Precipitation:
695 Beyond Paleothermometry. *Reviews in Mineralogy and Geochemistry* 43, 527-553.
- 696 Bakke, J., Lie, O., Heegaard, E., Dokken, T., Haug, G.H., Birks, H.H., Dulski, P. and Nilsen, T. (2009)
697 Rapid oceanic and atmospheric changes during the Younger Dryas cold period. *Nature Geoscience* 2,
698 202-205.
- 699 Barbour, M.M. (2007) Stable oxygen isotope composition of plant tissue: a review. *Funct. Plant Biol.*
700 34, 83-94.

- 701 Blaga, C.I., Reichart, G.J., Lotter, A.F., Anselmetti, F.S. and Damste, J.S.S. (2013) A TEX86 lake
702 record suggests simultaneous shifts in temperature in Central Europe and Greenland during the last
703 deglaciation. *Geophysical Research Letters* 40, 948-953.
- 704 Bowen, G.J. (2008) Spatial analysis of the intra-annual variation of precipitation isotope ratios and its
705 climatological corollaries. *J. Geophys. Res.-Atmos.* 113.
- 706 Brauer, A., Endres, C., Günter, C., Litt, T., Stebich, M. and Negendank, J.F.W. (1999a) High resolution
707 sediment and vegetation responses to Younger Dryas climate change in varved lake sediments from
708 Meerfelder Maar, Germany. *Quaternary Science Reviews* 18, 321-329.
- 709 Brauer, A., Endres, C. and Negendank, J.F.W. (1999b) Lateglacial calendar year chronology based on
710 annually laminated sediments from Lake Meerfelder Maar, Germany. *Quaternary International* 61, 17-
711 25.
- 712 Brauer, A., Haug, G.H., Dulski, P., Sigman, D.M. and Negendank, J.F.W. (2008) An abrupt wind shift
713 in western Europe at the onset of the Younger Dryas cold period. *Nature Geoscience* 1, 520-523.
- 714 Bremer, K. and Humphries, C.J. (1993) *Generic Monograph of the Asteraceae-Anthemideae*. The
715 Natural History Museum.
- 716 Bush, R.T. and McInerney, F.A. (2013) Leaf wax n-alkane distributions in and across modern plants:
717 Implications for paleoecology and chemotaxonomy. *Geochimica et Cosmochimica Acta* 117, 161-179.
- 718 Center for Sustainability and the Global Environment (SAGE) (2002) *Atlas of the biosphere - Average*
719 *Annual Relative Humidity* - <http://www.sage.wisc.edu>. Nelson Institute for Environmental
720 Studies - University of Wisconsin, The Board of Regents of the University of Wisconsin System.
- 721 Craig, G.L. (1965) Deuterium and oxygen 18 variations in the ocean and the marine atmosphere, in:
722 Tongioli, E. (Ed.), *Stable Isotopes in Oceanographic Studies and Paleotemperatures*. CNR Lab. Geol.
723 Nucl., Pisa, pp. 9-130.
- 724 D'Andrea, S., Caramiello, R., Ghignone, S. and Siniscalco, C. (2003) Systematic studies on some
725 species of the genus *Artemisia*: biomolecular analysis. *Plant Biosystems - An International Journal*
726 *Dealing with all Aspects of Plant Biology* 137, 121-130.
- 727 Dawson, T.E. (1993) Hydraulic lift and water-use by plants - Implications for water-balance,
728 performance and plant-plant interactions. *Oecologia* 95, 565-574.
- 729 Diefendorf, A.F., Freeman, K.H., Wing, S.L. and Graham, H.V. (2011) Production of n-alkyl lipids in
730 living plants and implications for the geologic past. *Geochimica et Cosmochimica Acta* 75, 7472-7485.
- 731 Dongmann, G., Nurnberg, H.W., Forstel, H. and Wagener, K. (1974) Enrichment of H₂¹⁸O in leaves
732 of transpiring plants. *Radiation and Environmental Biophysics* 11, 41-52.
- 733 Eglinton, G. and Hamilton, R.J. (1967) Leaf epicuticular waxes. *Science* 156, 1322-1327.
- 734 Farquhar, G.D. and Cernusak, L.A. (2005) On the isotopic composition of leaf water in the non-steady
735 state. *Funct. Plant Biol.* 32, 293-303.
- 736 Farquhar, G.D., Cernusak, L.A. and Barnes, B. (2007) Heavy water fractionation during transpiration.
737 *Plant Physiol.* 143, 11-18.
- 738 Farquhar, G.D. and Lloyd, J. (1993) Carbon and Oxygen Isotope Effects in the Exchange of Carbon
739 Dioxide between Terrestrial Plants and the Atmosphere, in: Ehleringer, J.R., Hall, A.E., Farquhar, G.D.
740 (Eds.), *Stable Isotopes and Plant Carbon-water Relations*. Academic Press, San Diego, pp. 47-70.
- 741 Feakins, S.J. (2013) Pollen-corrected leaf wax D/H reconstructions of northeast African hydrological
742 changes during the late Miocene. *Paleogeogr. Paleoclimatol. Paleoecol.* 374, 62-71.

- 743 Ferrio, J.P., Cuntz, M., Offermann, C., Siegwolf, R., Saurer, M. and Gessler, A. (2009) Effect of water
744 availability on leaf water isotopic enrichment in beech seedlings shows limitations of current
745 fractionation models. *Plant Cell and Environment* 32, 1285-1296.
- 746 Ficken, K.J., Li, B., Swain, D.L. and Eglinton, G. (2000) An n-alkane proxy for the sedimentary input
747 of submerged/floating freshwater aquatic macrophytes. *Organic Geochemistry* 31, 745-749.
- 748 Gamarra, B., Sachse, D. and Kahmen, A. (2016) Effects of leaf water evaporative 2H-enrichment and
749 biosynthetic fractionation on leaf wax n-alkane $\delta^2\text{H}$ values in C3 and C4 grasses. *Plant, Cell &*
750 *Environment*.
- 751 Gao, L., Hou, J., Toney, J., MacDonald, D. and Huang, Y. (2011) Mathematical modeling of the
752 aquatic macrophyte inputs of mid-chain n-alkyl lipids to lake sediments: Implications for interpreting
753 compound specific hydrogen isotopic records. *Geochimica et Cosmochimica Acta* 75, 3781-3791.
- 754 Gat, J.R. (1996) Oxygen and Hydrogen isotopes in the hydrologic cycle. *Annual Review of Earth and*
755 *Planetary Sciences* 24, 225-262.
- 756 Goslar, T., Arnold, M. and Pazdur, M.F. (1995) The Younger Dryas cold event - was it synchronous
757 over the North-Atlantic region. *Radiocarbon* 37, 63-70.
- 758 Goslar, T., Kuc, T., Ralska-Jasiewiczowa, M., R \geq z ν nski, K., Arnold, M., Bard, E., van Geel, B.,
759 Pazdur, M.Ç., Szeroczyńska, K., Wicik, B.Ç., Wiśniewski, K. and Walanus, A. (1993) High-
760 resolution lacustrine record of the late glacial/holocene transition in central Europe. *Quaternary Science*
761 *Reviews* 12, 287-294.
- 762 Heiri, O., Brooks, S.J., Renssen, H., Bedford, A., Hazekamp, M., Ilyashuk, B., Jeffers, E.S., Lang, B.,
763 Kirilova, E., Kuiper, S., Millet, L., Samartin, S., Toth, M., Verbruggen, F., Watson, J.E., van Asch, N.,
764 Lammertsma, E., Amon, L., Birks, H.H., Birks, H.J.B., Mortensen, M.F., Hoek, W.Z., Magyari, E.,
765 Muñoz Sobrino, C., Seppä, H., Tinner, W., Tonkov, S., Veski, S. and Lotter, A.F. (2014) Validation of
766 climate model-inferred regional temperature change for late-glacial Europe. *Nat Commun* 5.
- 767 Heiri, O., Cremer, H., Engels, S., Hoek, W.Z., Peeters, W. and Lotter, A.F. (2007) Lateglacial summer
768 temperatures in the Northwest European lowlands: a chironomid record from Hijkermeer, the
769 Netherlands. *Quaternary Science Reviews* 26, 2420-2437.
- 770 Hoek, W. (2009) Bølling-Allerød Interstadial, in: Gornitz, V. (Ed.), *Encyclopedia of Paleoclimatology*
771 *and Ancient Environments*. Springer Netherlands, pp. 100-103.
- 772 IAEA/WMO (2006) Global Network of Isotopes in Precipitation. The GNIP Database, Bundesanstalt
773 fuer Gewaesserkunde.
- 774 IPCC (2015) Intergovernmental panel on climate change, <http://www.IPCC.ch>.
- 775 Jackson, R.B., Canadell, J., Ehleringer, J.R., Mooney, H.A., Sala, O.E. and Schulze, E.D. (1996) A
776 global analysis of root distributions for terrestrial biomes. *Oecologia* 108, 389-411.
- 777 Jacob, H. and Sonntag, C. (1991) An 8-year record of the seasonal-variation of H-2 and O-18 in
778 atmospheric water-vapor and precipitation at Heidelberg, Germany. *Tellus Series B-Chemical and*
779 *Physical Meteorology* 43, 291-300.
- 780 Jacob, J., Huang, Y., Disnar, J.-R., Sifeddine, A., Boussafir, M., Spadano Albuquerque, A.L. and
781 Turcq, B. (2007) Paleohydrological changes during the last deglaciation in Northern Brazil. *Quaternary*
782 *Science Reviews* 26, 1004-1015.
- 783 Jasechko, S., Sharp, Z.D., Gibson, J.J., Birks, S.J., Yi, Y. and Fawcett, P.J. (2013) Terrestrial water
784 fluxes dominated by transpiration. *Nature* 496, 347-+.

- 785 Jones, H.G. (2013) *Plants and Microclimate: A Quantitative Approach to Environmental Plant*
786 *Physiology*. Cambridge University Press.
- 787 Kahmen, A., Dawson, T.E., Vieth, A. and Sachse, D. (2011a) Leaf wax n-alkane delta D values are
788 determined early in the ontogeny of *Populus trichocarpa* leaves when grown under controlled
789 environmental conditions. *Plant Cell and Environment* 34, 1639-1651.
- 790 Kahmen, A., Hoffmann, B., Schefuss, E., Arndt, S.K., Cernusak, L.A., West, J.B. and Sachse, D.
791 (2013a) Leaf water deuterium enrichment shapes leaf wax n-alkane delta D values of angiosperm
792 plants II: Observational evidence and global implications. *Geochimica et Cosmochimica Acta* 111, 50-
793 63.
- 794 Kahmen, A., Sachse, D., Arndt, S.K., Tu, K.P., Farrington, H., Vitousek, P.M. and Dawson, T.E.
795 (2011b) Cellulose delta(18)O is an index of leaf-to-air vapor pressure difference (VPD) in tropical
796 plants. *Proceedings of the National Academy of Sciences* 108, 1981-1986.
- 797 Kahmen, A., Schefuss, E. and Sachse, D. (2013b) Leaf water deuterium enrichment shapes leaf wax n-
798 alkane delta D values of angiosperm plants I: Experimental evidence and mechanistic insights.
799 *Geochimica et Cosmochimica Acta* 111, 39-49.
- 800 Kahmen, A., Simonin, K., Tu, K., Goldsmith, G.R. and Dawson, T.E. (2009) The influence of species
801 and growing conditions on the 18-O enrichment of leaf water and its impact on 'effective path length'.
802 *New Phytologist* 184, 619-630.
- 803 Kanner, L.C., Burns, S.J., Cheng, H., Edwards, R.L. and Vuille, M. (2013) High-resolution variability
804 of the South American summer monsoon over the last seven millennia: insights from a speleothem
805 record from the central Peruvian Andes. *Quaternary Science Reviews* 75, 1-10.
- 806 Klein, T. (2014) The variability of stomatal sensitivity to leaf water potential across tree species
807 indicates a continuum between isohydric and anisohydric behaviours. *Functional Ecology* 28, 1313-
808 1320.
- 809 Leuzinger, S. and Korner, C. (2007) Tree species diversity affects canopy leaf temperatures in a mature
810 temperate forest. *Agricultural and Forest Meteorology* 146, 29-37.
- 811 Litt, T. and Stebich, M. (1999) Bio- and chronostratigraphy of the lateglacial in the Eifel region,
812 Germany. *Quaternary International* 61, 5-16.
- 813 Moschen, R., Lucke, A. and Schleser, G.H. (2005) Sensitivity of biogenic silica oxygen isotopes to
814 changes in surface water temperature and palaeoclimatology. *Geophysical Research Letters* 32.
- 815 New, M., Hulme, M. and Jones, P. (1999) Representing Twentieth-Century Space-Time Climate
816 Variability. Part I: Development of a 1961-90 Mean Monthly Terrestrial Climatology. *Journal of*
817 *Climate* 12, 829-856.
- 818 Nichols, J.E., Walcott, M., Bradley, R., Pilcher, J. and Huang, Y. (2009) Quantitative assessment of
819 precipitation seasonality and summer surface wetness using ombrotrophic sediments from an Arctic
820 Norwegian peatland. *Quaternary Research* 72, 443-451.
- 821 Peters, K.E., Moldovan, J.M. and Walters, C.C. (2007) *The Biomarker Guide: Volume 1, Biomarkers*
822 *and Isotopes in the Environment and Human History*. Cambridge University Press.
- 823 Rach, O., Brauer, A., Wilkes, H. and Sachse, D. (2014) Delayed hydrological response to Greenland
824 cooling at the onset of the Younger Dryas in western Europe. *Nature Geoscience* 7, 109-112.
- 825 Sachse, D., Billault, I., Bowen, G.J., Chikaraishi, Y., Dawson, T.E., Feakins, S.J., Freeman, K.H.,
826 Magill, C.R., McInerney, F.A., van der Meer, M.T.J., Polissar, P., Robins, R.J., Sachs, J.P., Schmidt,
827 H.-L., Sessions, A.L., White, J.W.C., West, J.B. and Kahmen, A. (2012) Molecular Paleohydrology:
828 Interpreting the Hydrogen-Isotopic Composition of Lipid Biomarkers from Photosynthesizing
829 Organisms. *Annual Review of Earth and Planetary Sciences* 40, 221-249.

- 830 Sachse, D., Dawson, M.N. and Kahmen, A. (2015) Seasonal variation of leaf wax n-alkane production
831 and $\delta^2\text{H}$ values from the evergreen oak tree, *Quercus agrifolia*. *Isotopes in Environmental & Health*
832 *Studies in press*.
- 833 Sachse, D., Kahmen, A. and Gleixner, G. (2009) Significant seasonal variation in the hydrogen isotopic
834 composition of leaf-wax lipids for two deciduous tree ecosystems (*Fagus sylvatica* and *Acer*
835 *pseudoplatanus*). *Organic Geochemistry* 40, 732-742.
- 836 Sachse, D., Radke, J. and Gleixner, G. (2004) Hydrogen isotope ratios of recent lacustrine sedimentary
837 n-alkanes record modern climate variability. *Geochimica et Cosmochimica Acta* 68, 4877-4889.
- 838 Sachse, D., Radke, J. and Gleixner, G. (2006) δD values of individual n-alkanes from terrestrial plants
839 along a climatic gradient - Implications for the sedimentary biomarker record. *Organic Geochemistry*
840 37, 469-483.
- 841 Schefuss, E., Kuhlmann, H., Mollenhauer, G., Prange, M. and Pätzold, J. (2011) Forcing of wet phases
842 in southeast Africa over the past 17,000 years. *Nature* 480, 509-512.
- 843 Scherrer, D., Bader, M.K.F. and Korner, C. (2011) Drought-sensitivity ranking of deciduous tree
844 species based on thermal imaging of forest canopies. *Agricultural and Forest Meteorology* 151, 1632-
845 1640.
- 846 Schulze, E.D. (1986) Carbon dioxide and water vapor exchange in response to drought in the
847 atmosphere and in the soil. *Annual Review of Plant Physiology and Plant Molecular Biology* 37, 247-
848 274.
- 849 Schulze, E.D., Hall, A. E. (1982) Stomatal response, water loss and CO_2 assimilation rates of plants in
850 contrasting environments. *Encyclopedia of Plant Physiology* 12B, 181-230.
- 851 Schwark, L., Zink, K. and Lechterbeck, J. (2002) Reconstruction of postglacial to early Holocene
852 vegetation history in terrestrial Central Europe via cuticular lipid biomarkers and pollen records from
853 lake sediments. *Geology* 30, 463-466.
- 854 Seki, O., Meyers, P.A., Yamamoto, S., Kawamura, K., Nakatsuka, T., Zhou, W. and Zheng, Y. (2011)
855 Plant-wax hydrogen isotopic evidence for postglacial variations in delivery of precipitation in the
856 monsoon domain of China. *Geology* 39, 875-878.
- 857 Sessions, A.L. and Hayes, J.M. (2005) Calculation of hydrogen isotopic fractionations in
858 biogeochemical systems. *Geochimica et Cosmochimica Acta* 69, 593-597.
- 859 Smith, F.A. and Freeman, K.H. (2006) Influence of physiology and climate on delta D of leaf wax n-
860 alkanes from C-3 and C-4 grasses. *Geochimica Et Cosmochimica Acta* 70, 1172-1187.
- 861 Song, X., Barbour, M.M., Farquhar, G.D., Vann, D.R. and Helliker, B.R. (2013) Transpiration rate
862 relates to within- and across-species variations in effective path length in a leaf water model of oxygen
863 isotope enrichment. *Plant Cell and Environment* 36, 1338-1351.
- 864 Tipple, B.J., Berke, M.A., Doman, C.E., Khachatryan, S. and Ehleringer, J.R. (2013) Leaf-wax n-
865 alkanes record the plant-water environment at leaf flush. *Proceedings of the National Academy of*
866 *Sciences* 110, 2659-2664.
- 867 Turner, N.C., Schulze, E. D., & Gollan, T. (1984) The responses of stomata and leaf gas exchange to
868 vapour pressure deficits and soil water content. *Oecologia* 63(3), 338-342.
- 869 Tyler, J.J., Leng, M.J., Sloane, H.J., Sachse, D. and Gleixner, G. (2008) Oxygen isotope ratios of
870 sedimentary biogenic silica reflect the European transcontinental climate gradient. *Journal of*
871 *Quaternary Science* 23, 341-350.
- 872 von Grafenstein, U., Erlenkeuser, H., Brauer, A., Jouzel, J. and Johnsen, S.J. (1999) A mid-European
873 decadal isotope-climate record from 15,500 to 5000 years BP. *Science* 284, 1654-1657.

- 874 Wang, Y.V., Larsen, T., Leduc, G., Andersen, N., Blanz, T. and Schneider, R.R. (2013) What does leaf
875 wax δD from a mixed C3/C4 vegetation region tell us? *Geochimica et Cosmochimica Acta* 111, 128-
876 139.
- 877 Zhang, X.N., Gillespie, A.L. and Sessions, A.L. (2009) Large D/H variations in bacterial lipids reflect
878 central metabolic pathways. *Proc. Natl. Acad. Sci. U. S. A.* 106, 12580-12586.
- 879 Zhang, Z. and Sachs, J.P. (2007) Hydrogen isotope fractionation in freshwater algae: I. Variations
880 among lipids and species. *Organic Geochemistry* 38, 582-608.
881
882